

# HATPRO MWR rain flagging and radome status monitoring

Moritz Löffler

October 2022

## 1 Introduction

Microwave radiometers (**MWR**) are moving into the focus of national and trans-national meteorological agencies which already operate or which intend to deploy MWR in network setups. The centralized processing of MWR data products within ACTRIS<sup>1</sup> and the imminent integration of MWR into the EUMETNET<sup>2</sup> E-Profile<sup>3</sup> network are two prominent examples for this development. The developments within E-Profile correspond to efforts made by national weather services towards assimilating MWR brightness temperature ( $T_B$ ) data.

One precondition for a successful deployment will be automatic data quality checks and a technical monitoring. E.g. MWR observations are biased during precipitation. This effect increases when weathering effects diminish the hygroscopic properties of the protective radome. A continuous flagging of data biased due to precipitation and a monitoring of the hygroscopic properties of the radome will benefit data quality and availability of operational MWR.

In this document we evaluate and discuss existing rain bias mitigation strategies of the HATPRO MWR and demonstrate the impact of undetected rain on the observation. We introduce complementary rain bias mitigation strategies and a monitoring tool for the radome hygroscopic properties. This tool is available under [https://github.com/moritzloeffler/mwr\\_radome](https://github.com/moritzloeffler/mwr_radome). HDCP<sup>2</sup> (SAMD) and E-PROFILE data formats can be processed. For more information please refer to the online documentation.

This fits well into the objective O4.1 of Probe to improve the quality and maturity of atmospheric boundary layer (**ABL**) profiling. And it contributes to the action deliverables D4.1 and D3.3.

### 1.1 Theoretical background

MWR are passive remote sensors and record the thermal emissions of the atmosphere most popularly in the K-band (21 GHz to 31 GHz) and in the V-band (51 GHz to 58 GHz). As

---

<sup>1</sup>The Aerosol, Clouds and Trace Gases Research Infrastructure - [www.actris.net](http://www.actris.net)

<sup>2</sup>European Meteorological Network, <https://www.eumetnet.eu/>

<sup>3</sup>EUMETNET Profiling Programme (wind observations from weather radars and dedicated wind profilers and Lidar/Ceilometer observations)

long as the recorded signal originates from the thermal emission and absorption of atmospheric gases and cloud particles the thermodynamic state of the atmosphere can be approximated using inverse radiative transfer modelling. Water on the radome [5, 1] and scattering processes on atmospheric rain droplets [4] are not accounted for by common retrieval algorithms and respective radiative transfer models. Consequently, precipitation leads to biased retrievals.

If there is no liquid water on the radome the MWR will observe the downwelling spectral radiances emitted by the atmosphere above. These spectral radiances and the resulting  $T_B$  typically vary significantly between the channels due to the different spectral absorption coefficients (Fig. 1). A bias in the observed  $T_B$  resulting from liquid water on the radome is easily above a few Kelvin and thus well outside the instrument uncertainty [see VMG contribution from T. Böck]. In the limit of a thick layer of liquid water which absorbs and reflects all radiance of atmospheric origin, the observed  $T_B$  will equal the radome temperature. The radome temperature is expected to be slightly above or equal the ambient temperature.

In the existing configuration of channels there is a strong correlation between  $T_B$ -observations

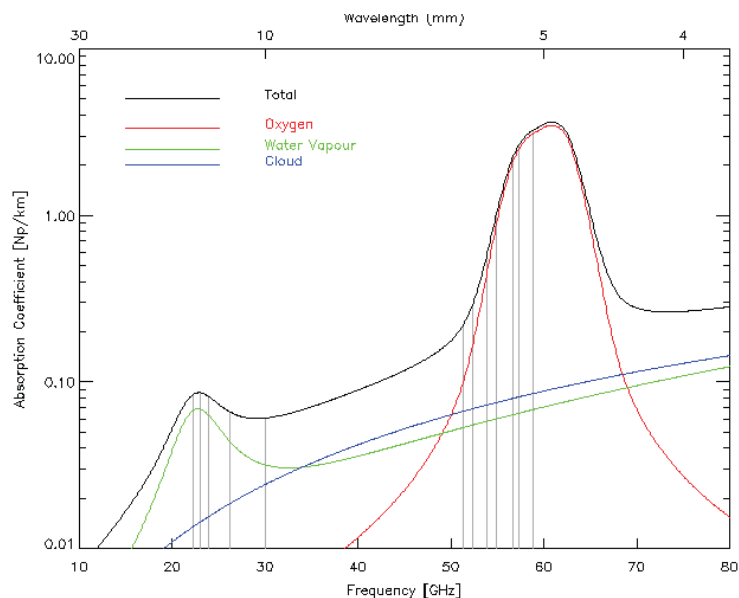


Figure 1: *Constitution of the overall absorption coefficient in a typical atmospheric state and presence of a thin liquid water cloud.*

in neighbouring channels. This correlation has some predictive power when assuming an atmospheric origin of the signal. Such a prediction (spectral retrieval) was implemented by the instrument producer Radiometer Physics (**RPG**). The details are not public, the general procedure, however, is known. A neural network is trained on a long time series of  $T_B$  computed from radiosonde ascents with a radiative transfer model. This neural network predicts the  $T_B$  of any frequency within the K- and V-band using a subset of the available observations.

If the radome is wet, the spectral retrieval cannot reproduce the observed spectrum, as it is inconsistent with any possible atmospheric condition. This leads to biases between the obser-

vation and the spectral retrieval. The bias between the observation and the spectral retrieval at  $53.9\text{ GHz}$  is an especially stable indicator for detecting spectral inconsistencies due to liquid water on the radome.

## 1.2 Description of data used in study

In the MWR data of the case studies was collected during the FESSTVaL field campaign and is published under DOI 10.25592/uhhfdm.10197 [2]. This MWR data includes the level-1  $T_B$  and in-situ observations as well as the derived level-2 products, e.g. the spectral retrieval (SPC).

The MWR observations and retrievals used for statistical evaluations are also located at the observatory in Lindenberg. They are not published at the time. Starting 2022, the data is freely available on the below mentioned CloudNet data server.

The disdrometer observations are included in the CloudNet categorize dataset of Lindenberg. The CloudNet categorize and target classification timeseries can be retrieved from an API. More information on the how and what can be found at <https://cloudnet.fmi.fi/>.

## 2 Default mitigation strategies and their performance

As the MWR community is long aware of biases induced by a wet radome, strategies are in place which prevent the unnoticed collection and use of biased data.

Most importantly, the radome is coated with a hygroscopic layer, which decreases accumulation of water. In combination with a heater blower, which is activated when rain is detected and above a relative humidity threshold, the biasing effect of precipitation is minimized.

For precipitation detection the HATPRO G5 MWR is equipped with a Vaisala®WXT536 weather station. The WXT536 measures precipitation with a piezoelectric precipitation sensor [3], which registers rainfall by sensing the impact of the drops on a membrane. Any data collected in this situation is flagged as not-usable. Very small drop sizes, e.g. drizzle, are detected less likely, the limit seems to be at around  $0.5\text{ mm/h}$  (see fig. 2). The sensitivity likely depends more on the drop size distribution than the rain rate.

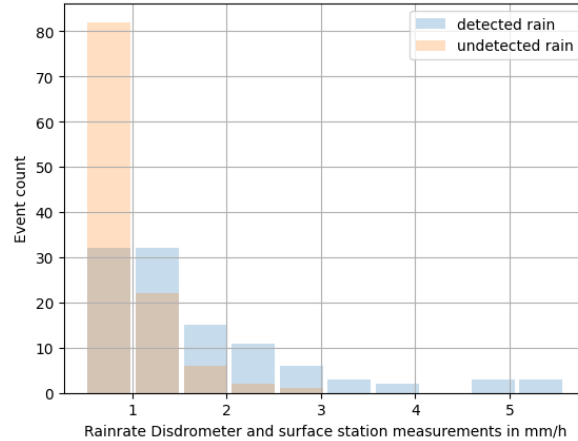


Figure 2: Histogram of rain detected and undetected by the HATPRO precipitation sensor for rain rates below  $1 \text{ mm/h}$  observed by the ACTRIS CloudNet disdrometer at the DWD observatory in Lindenberg. The evaluation contains observations once per hour between Oct. 2020 and Feb. 2022.

Evaluations of MWR observations and the retrievals showed that observations at  $75^\circ$  elevation significantly reduce bias and rms of the resulting retrievals during precipitation events [6, 7]. Additionally to the beforementioned preinstalled mitigation strategies a number of good practice and technical monitoring recommendations were published during a prior Cost Action under [http://cfa.aquila.infn.it/wiki.eg-climet.org/index.php5/MWR\\_Technical\\_Implementation](http://cfa.aquila.infn.it/wiki.eg-climet.org/index.php5/MWR_Technical_Implementation).

## 2.1 Effect of rain when the radome is new

The recommendation is to install a new radome at least every six months or sooner if weathering effects are visible. A well maintained MWR is capable of making high-quality observations in situations with light rain and drizzle. The heater-blower should be activated by the high relative humidity and should prevent accumulation of water on the radome [HATRPO brochure]. The following examples illustrate the effect of rain on the  $T_B$  observations in case of a newly installed radome. The radome was mounted on May 1st 2021 at the begin of the FESSTVaL campaign. The comparison of observation and spectral retrieval reveals that even in case of rain rates above  $5 \text{ mm/h}$  the bias does not exceed  $2 \text{ K}$  (Fig.4). In case of drizzle (Fig.3) no effect on the  $T_B$  at  $53.9 \text{ GHz}$  becomes apparent. The rain in this case was so light, that it went mostly unnoticed by precipitation sensor.

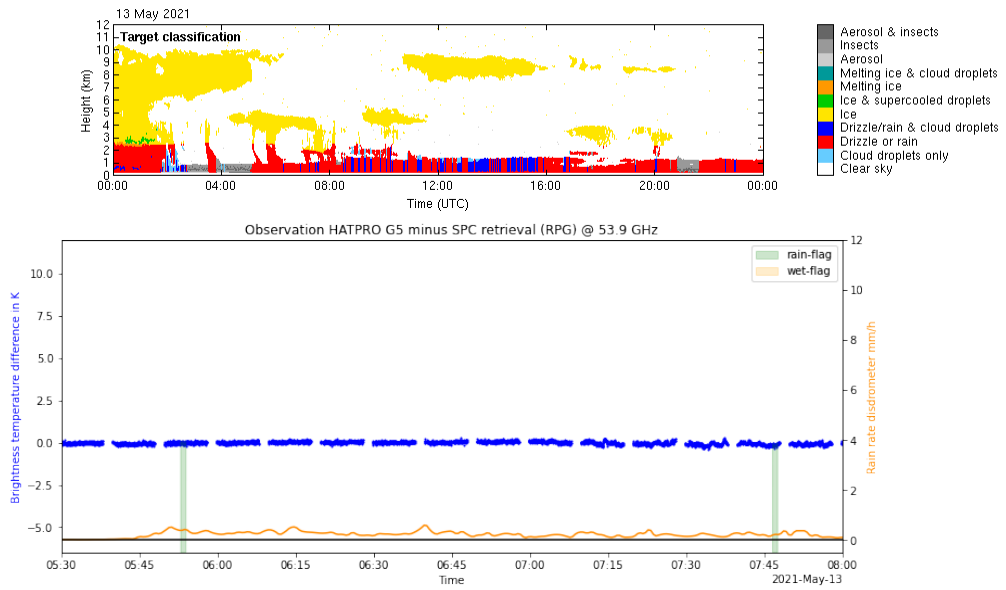


Figure 3: *Bottom: Observation minus SPC-retrieval (blue) of HATPRO G5 at Lindenberg during an event with drizzle. The rain rate is in orange. Rain events noticed by the precipitation sensor are marked in green. Top: The CloudNet target classification for that day.*

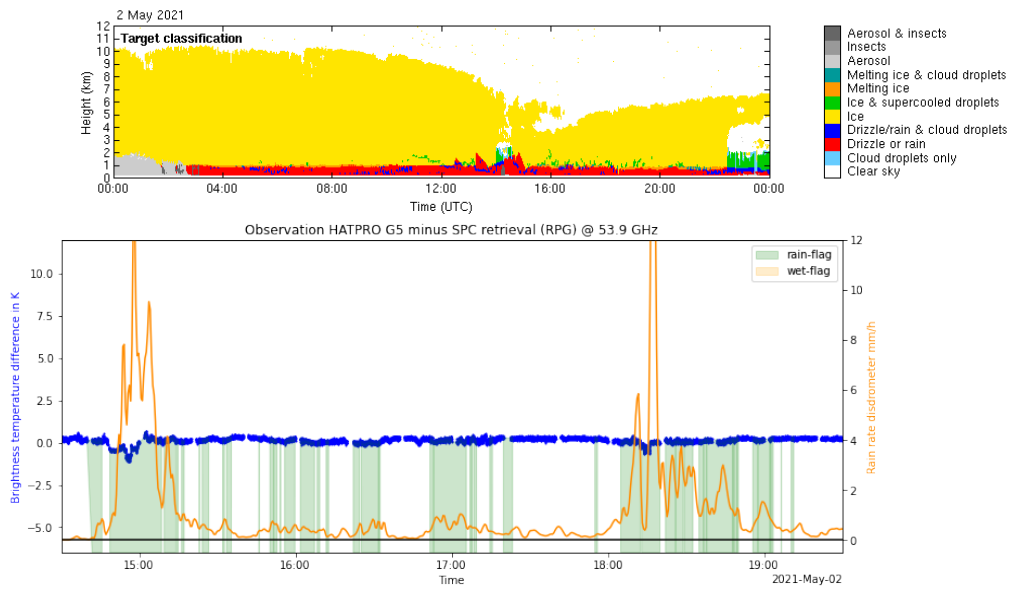


Figure 4: *Bottom: Observation minus SPC-retrieval (blue) of HATPRO G5 at Lindenberg during an event with rain. The rain rate is in orange. Rain events noticed by the precipitation sensor are marked in green. Top: The CloudNet target classification for that day.*

## 2.2 Effect of rain if radome has undergone weathering

Towards the end of its lifetime the radome will lose its hygroscopic properties. Especially during extended rain events the biasing effect of the water increases with the duration of the rain. Similar to a hysteresis effect, after the end of the rain, it takes some time for the bias to decrease back towards zero. We consider the radome to be wet in these situations.

The two following case studies were performed on the same day. In the morning hours there was a situation with drizzle and in the afternoon and evening there was a rain event which lasted longer and had higher rain rates. The radome is 4 months old at this time.

The drizzle in the morning hours (fig. 5) has no apparent effect on the  $T_B$  at 53.9 GHz. However, the rain in the evening leads to large biases in the  $T_B$ . This bias takes some time to build up in the beginning and steadily increases to a maximum around 12 K in the 53.9 GHz channel. After the end of the rain event and during interruptions the bias only slowly decreases. The observations during these interruptions and during the time it takes to dry are not automatically flagged.

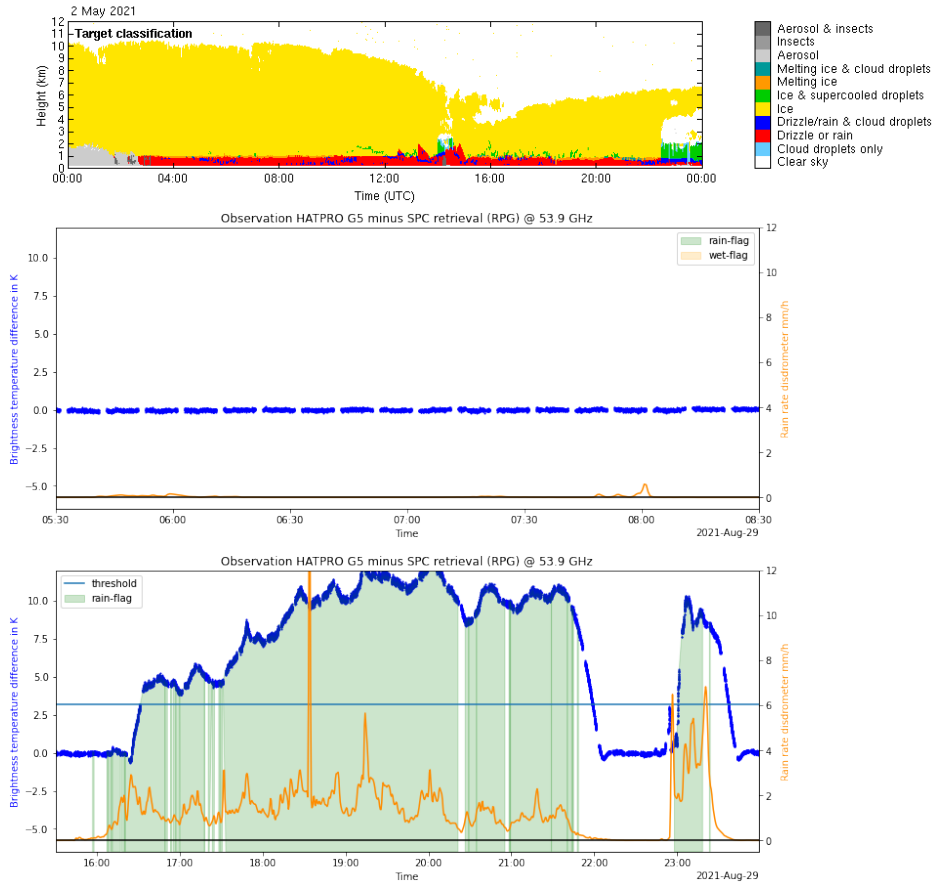


Figure 5: Observation minus SPC-retrieval (blue) of HATPRO G5 at Lindenberg during an event with drizzle (middle) and rain (bottom). The rainrate is in orange. Rain events noticed by the precipitation sensor are marked in green. The CloudNet target classification for that day is displayed above.

When looking at the resulting retrievals of integrated water vapor and temperature profiles (Fig. 6), the possible effect of including such biased  $T_B$ -observations in product generation becomes evident. The consecutive retrievals display a strong variation, which does not reflect a plausible atmospheric process. The effect of precipitation on the resulting retrievals has been discussed extensively in past publications e.g. [5, 7].

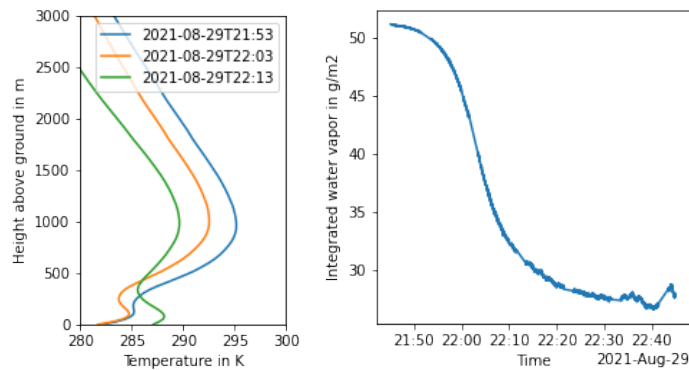


Figure 6: *Temperature profiles (left) and integrated water vapor (right) retrieved during and after the evening rain-event on August 29, 2021*

### 3 Additional mitigation strategies

The aging of the radome cannot be foreseen for every possible scenario and maintenance can be delayed or unknown when working with a foreign dataset. These common scenarios necessitate additional mitigation strategies to avoid using biased data and compromising data products or use cases such as data assimilation.

#### 3.1 Observation minus spectral retrieval

The spectral retrieval is a quite useful tool for monitoring the presence of a liquid water layer on the radome. Spectral inconsistencies immediately after a rain-event can be attributed to a liquid water layer on the radome.

Section 1.1 mentions that  $T_B$  at  $53.9\text{ GHz}$  is most suitable for detecting biases caused by a liquid layer on the radome. A dynamically determined threshold,  $2\text{ K}$  above the average difference between observation and retrieval at  $53.9\text{ GHz}$ , triggers the end of the time-to-dry. The resulting wet-flag, before the end of the time-to-dry, is marked orange in figure 7 and figure 8. In this manner the wet-flag accounts for gaps in the precipitation sensor-flagging and the drying process after a precipitation event.

It is important to note that the match between observation and spectral retrieval is not always perfect and varies slightly. To account for this variability the threshold is determined dynamically. With the described method, large amounts of undetected rain will lead to a higher threshold and therefore a shortened time-to-dry.

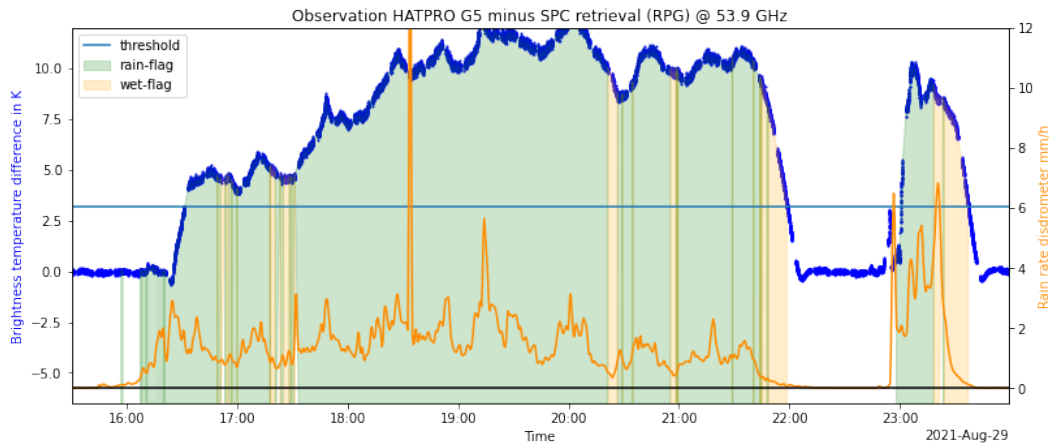


Figure 7: Observation minus SPC-retrieval (blue) of HATPRO G5 at Lindenberg during a precipitation event. The rainrate is in orange. Rain events noticed by the precipitation sensor are marked in green, gaps filled with spectral retrieval method and the time-to-dry are marked in orange

### 3.2 Additional buffer time at the end of rain event

To complement the wet-flagging and capture any questionable data the wet-flag can be extended for an additional time after the flagging with the spectral retrieval ended. The time required here depends on the duration of the rain and the condition of the radome as well as the ambient weather (Temperature, humidity, sun, wind).

An average drying rate results in a linear decrease of the bias by around  $1 K/180 s$ . With this average value and the observation minus spectral retrieval the additional buffer time is easily calculated. The observations additionally flagged as wet are marked in blue in figure 8.

This approach is a stable and fairly simple possibility to flag biased data without excessively flagging unbiased data.



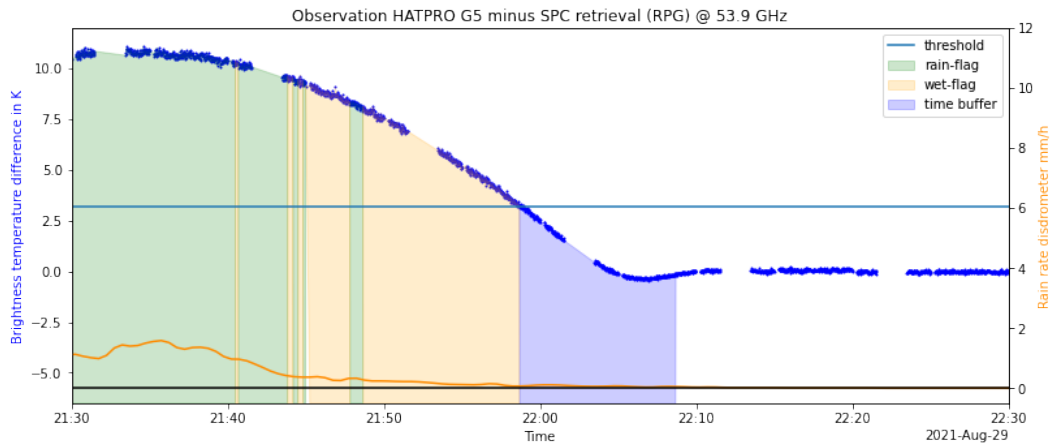


Figure 8: Zoom into figure 7. Observation minus SPC-retrieval (blue) of HATPRO G5 at Lindenberg during a precipitation event. The rainrate is in orange. Rain events noticed by the precipitation sensor are marked in green, gaps filled with spectral retrieval method and the time-to-dry are marked in orange, data flagged by the additional time buffer are marked in blue.

### 3.3 Replacing the radome

The examples in chapter 2 show that a well-maintained radiometer with a fairly new radome will benefit the availability of unbiased high-quality data. Chapter 4 will illustrate a possibility to monitor the hygroscopic properties of a radome without physical presence at the site. Apart from that every site may have specific circumstances leading to weathering of the radome. Examples are solar irradiation, salt, dirt and birds (see [http://cfa.aquila.infn.it/wiki.eg-climet.org/index.php5/MWR\\_Technical\\_Implementation](http://cfa.aquila.infn.it/wiki.eg-climet.org/index.php5/MWR_Technical_Implementation)).

Apart from the radome condition, the functionality of the heater blower should be checked regularly and the precipitation sensor should be kept clean. Details can be found in the manufacturers handbook.

When maintaining a site for a longer time it may be possible to identify anything out of the ordinary and adapt the maintenance schedule and the protective measures accordingly. E.g. the radome monitoring at the observatory in Lindenberg revealed that the radome frequently required maintenance at the end of summer.

## 4 Monitoring the radome condition

As mentioned in 3.3 the lifetime of the hygroscopic coating of a radome can vary significantly. A radome monitoring can be implemented with the time-to-dry (see 3.1) as an indicator for the condition of the hygroscopic coating. The monitoring of the hygroscopic condition of the radome should be favoured over a regular schedule, as it will benefit data quality and availability in the one case and save money in the other.

The tool for flagging and monitoring is available under <https://github.com/moritzloeffler/>

`mwr_radome`. HDCP<sup>2</sup> (SAMD) and E-PROFILE data formats can be processed. For more information please refer to the online documentation.

Recordings of the time-to-dry show that, once it emerges it steadily increases (see fig. 9 and fig. 10). This demonstrates why it is a stable indicator. Other possible indicators such as the maximum or mean difference between observation and spectral retrieval are possible. However, they do not have the same predictive power. Also, the time-to-dry is directly linked to the data loss and thus more intuitive to use.

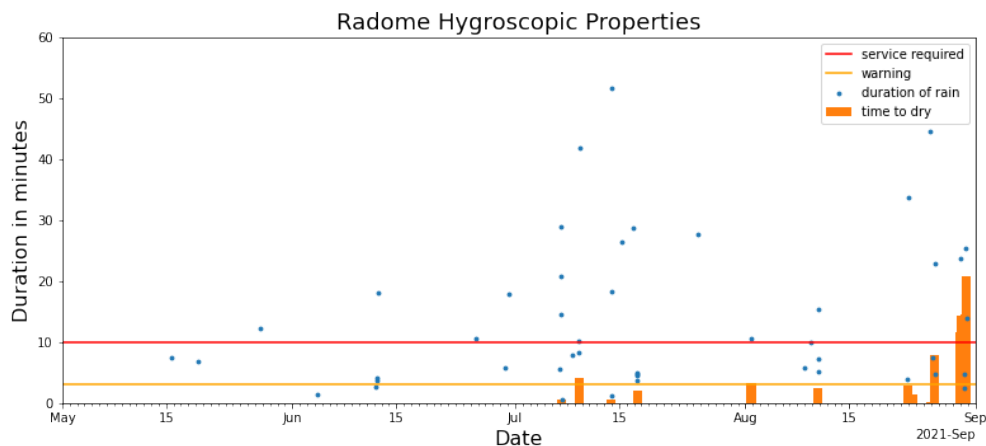


Figure 9: *Time-to-dry and duration-of-rain in minutes of the radome during the FESSTVaL campaign in Lindenberg 2021. The red and orange line indicate the threshold for issued warnings.*

Once certain thresholds for the “time-to-dry” are crossed for the first time an automatic warning can be issued. Each user can define these “time-to-dry”-thresholds according to their preferences regarding the data availability. The recommendation is to implement two limits. A good time to start planning for a radome exchange is when 3 minutes “time-to-dry” is exceeded for the first time. In this way maintenance can be performed shortly after 10 minutes “time-to-dry” is surpassed, a few weeks or months later.

After a few years it is possible to start exploring the onset of the weathering process and what reasons there could be. Figure 10 (top) illustrates how the life-time of a radome on the MWR can vary significantly. The life-time of the radome on the HATPRO at Lindenberg ranges from just over 100 days to almost one year. The bottom of figure 10 shows how there may be a pattern, which requires a new radome towards the end of summer. This pattern indicates UV-radiation as the main weathering factor. However, the data is not sufficient for a valid analysis and any assumptions about patterns and causality remain rather speculative.

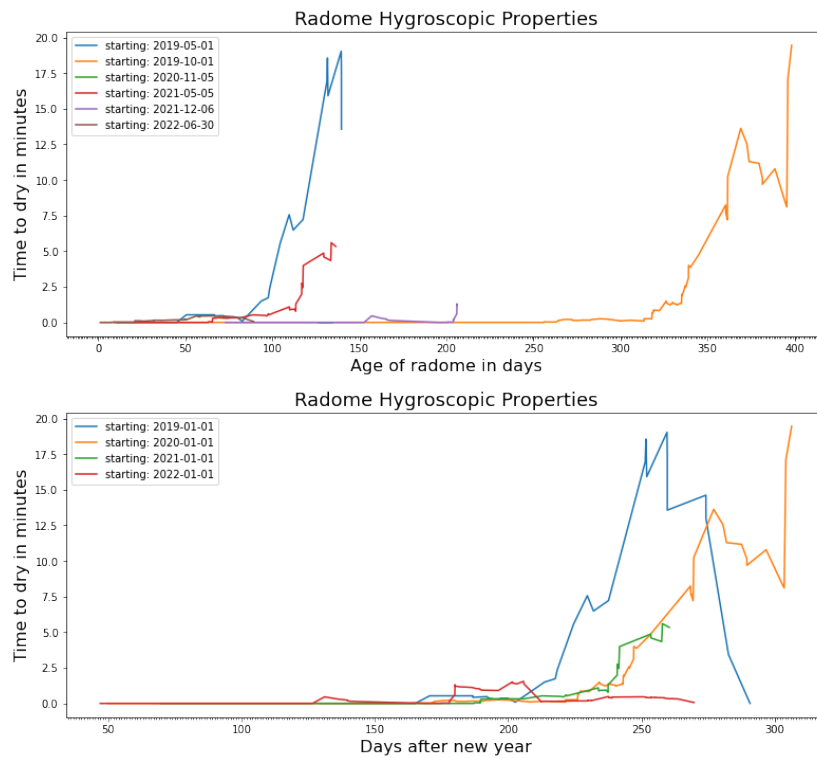


Figure 10: 30 day moving average of time-to-dry plotted against radome-age (top) and days of year(bottom).

## References

- [1] U Löhnert and O Maier. “Operational profiling of temperature using ground-based microwave radiometry at Payerne: Prospects and challenges”. In: *Atmospheric Measurement Techniques* 5.5 (2012), pp. 1121–1134. DOI: <https://doi.org/10.5194/amt-5-1121-2012>.
- [2] Ulrich Löhnert et al. *Microwave Radiometer Observations during FESSTVaL 2021*. Project: FESSTVaL (Field Experiment on submesoscale spatio-temporal variability in Lindenberg), a measurement campaign initiated by the Hans-Ertel-Center for Weather Research. May 2022. DOI: [10.25592/uhhfdm.10198](https://doi.org/10.25592/uhhfdm.10198). URL: <https://doi.org/10.25592/uhhfdm.10198>.
- [3] Atte Salmi et al. “Piezoelectric Vaisala raincap® rain sensor applied to drop size distribution monitoring”. In: *Technical Conference on Meteorological and Environmental Instruments and Methods of Observation*. World Meteorological Organization Geneva. 2011, pp. 1–7.
- [4] BE Sheppard. “Effect of rain on ground-based microwave radiometric measurements in the 20–90-GHz range”. In: *Journal of Atmospheric and Oceanic Technology* 13.6 (1996), pp. 1121–1134.

pp. 1139–1151. DOI: [https://doi.org/10.1175/1520-0426\(1996\)013%3C1139:EOROGB%3E2.0.CO;2](https://doi.org/10.1175/1520-0426(1996)013%3C1139:EOROGB%3E2.0.CO;2).

- [5] R Ware et al. “Ground-based microwave radiometer measurements during precipitation”. In: *8th Specialist Meeting on Microwave Radiometry*. 2004, pp. 24–27.
- [6] R. Ware et al. “Thermodynamic and liquid profiling during the 2010 Winter Olympics”. In: *Atmospheric Research* 132-133 (2013), pp. 278–290. ISSN: 0169-8095. DOI: <https://doi.org/10.1016/j.atmosres.2013.05.019>. URL: <https://www.sciencedirect.com/science/article/pii/S0169809513001737>.
- [7] Guirong Xu et al. “Effect of off-zenith observations on reducing the impact of precipitation on ground-based microwave radiometer measurement accuracy”. In: *Atmospheric Research* 140-141 (2014), pp. 85–94. ISSN: 0169-8095. DOI: <https://doi.org/10.1016/j.atmosres.2014.01.021>. URL: <https://www.sciencedirect.com/science/article/pii/S0169809514000234>.